Materials and Design 31 (2010) 1293–1301

Contents lists available at ScienceDirect

Materials and Design

journal homepage: www.elsevier.com/locate/matdes

Wire fence as applique armour

Sebastian Balos [a,*], Vencislav Grabulov [b], Leposava Sidjanin [a], Mladen Pantic [c]

[a] University of Novi Sad, Faculty of Technical Sciences, Department of Production Engineering, Trg D. Obradovica 6, 21000 Novi Sad, Serbia
[b] Institute for Materials Testing, Bulevar Vojvode Misica 43, 11000 Belgrade, Serbia
[c] Military Technical Institute, Ratka Resanovica 1, 11132 Belgrade, Serbia

ARTICLE INFO

Article history:
Received 30 June 2009
Accepted 6 September 2009
Available online 10 September 2009

Keywords:
A. Ferrous metals and alloys
E. Impact and ballistics
H. Failure analysis

ABSTRACT

In this paper, the behaviour of wire fence was investigated for potential as applique armour. The wire fence used was made from commercial high-strength patented wire and the supporting frames were made of mild steel L-profiles. Both patented wire and L-profiles are of-the-shelf materials. The fence was tested by firing 12.7 mm M8 API ammunition at four applique armour models: two of these models use a parallel wire arrangement, with one mounted at a 90° angle from the incoming projectile and the other at 70°; and two of these models use a zig-zag wire arrangement, one mounted at a firm 90° angle and the other is left in a hanging arrangement. Fence damage was correlated with RHA basic plate damage, on both the face and back. Wire fence has considerable potential as an improvised applique armour, except if the projectile impacts near the center of the wire or near the center between two wires. The latter case was successfully overcome by placing the armour model at an angle and by using a zig-zag wire arrangement. The lowest basic RHA plate damage level was found using the hanging armour model. However, from the point of view of ease of attachment, the most convenient was found to be the armour model with the zig-zag wire arrangement fixed at 90° angle from the incoming projectile. SEM fracto graphy revealed that the fracture surface was predominantly ductile, with dimples filled with debris from the incendiary effect of the projectile.

1. Introduction

The majority of Cold War era armour personnel carriers (APCs), infantry fighting vehicles (IFVs) and more recent mine–resistant ambush protected vehicles (MRAP) have the main portion of their armour designed to withstand 7.62 mm (7.62 × 51 and 7.62 × 54*R*) or 7.9 mm (7.9 × 57) armour-piercing (AP) ammunition, fired from battle rifles and machine guns [1]. The same ammunition is also considered to be the most dangerous threat for unarmoured trucks and logistic vehicles. Therefore, improvised armour of varying degrees of success is and will be a very common sight on trucks and logistics vehicles in any risky peace operation or low intensity conflict [2,3].

In the mean time, new threats have also emerged. In addition to heavy machine guns mounted on light SUVs, there are more anti-material rifles which fire basically the same 12.7 mm heavy machine gun ammunition (12.7 × 99 mm, 12.7 × 108 mm) and which have a tendency of wider proliferation as more Russian and Chinese designs appear. These rifles have considerably longer ranges, in excess of 1000 m, that makes them much more accurate and capable than anti-tank grenades in the form of rifle propelled grenades (RPG). In urban areas, their capability to fire from enclosed spaces makes anti-material rifles even more attractive to terrorists and insurgents. These larger calibers possess roughly three times the kinetic energy and twice the penetration compared to 7.62 and 7.9 mm ammunition [4,5].

Field modifications comprise the mounting of mild steel or rolled homogenous steel plates. These plates considerably limit the payload of a logistic vehicle. Therefore, a solution for increasing armour protection is needed, that will not add too much weight to the vehicle, but would increase its armour protection to the next level, and provide multi-hit resistance in the case of machine gun attack. Furthermore, it is very important to use locally or readily available resources and manufacturing processes. One very convenient way of making the projectile less effective is inducing yaw. As is widely reported, yaw may be induced even by a simple spaced armour [6]. This has been widely used during World War II, where a number of German tanks received mild steel add-on plates 5 and 8 mm thick, called *Shuerzen* [7,8]. This kind of applique armour packages were intended to make the sides of PzKpfw IV Ausf. G tanks immune to Soviet 14.5 mm PTRD and PTRS anti-tank rifles. Such modification ensured that 30 mm thick hull and turret sides became resistant to 14.5 mm B32 ammunition with penetration of 40 mm RHA at 100 m. However, a more effective solution was found among un homogenous armour types, such

* Corresponding author. Tel.: +381 214852339; fax: +381 454495.
E-mail address: sebab@uns.ns.ac.yu (S. Balos).

0261-3069/$ - see front matter © 2009 Elsevier Ltd. All rights reserved.
doi:10.1016/j.matdes.2009.09.013

as wire mesh, called *Thoma Schuerzen*. This has been used on German PzKpfw IV Ausf. J medium tanks, and consisted from a mild steel wire mesh. Wires were 5.5 mm thick, with a hole size of 13.5 mm [8].

In this paper, an attempt is made to investigate the possibility of using patented high tensile strength wire as a basic destabilizing element of an improvised applique armour. Patented wire is a widely available, off-the-shelf material used for reinforcing prestressed concrete structures [9,10]. The availability of patented wire is similar to other types of commercial steels, such as certain types of tool steels [11] and high-strength steels [12], useful when specialized armour steels are unavailable or in short supply. Various wire arrangements, angle of incident and add-on element mounting types are tested. This research may be one of the first papers in which the use of patented wire in the form of a fence is studied for ballistic protection as the authors of this paper are not aware of any other publications which address this in the open literature.

Table 1
Patented wire chemical composition.

C	Si	Mn	Cr	P	S	V	Fe
0.77	0.22	0.61	0.25	0.03	0.03	0.05	Balance

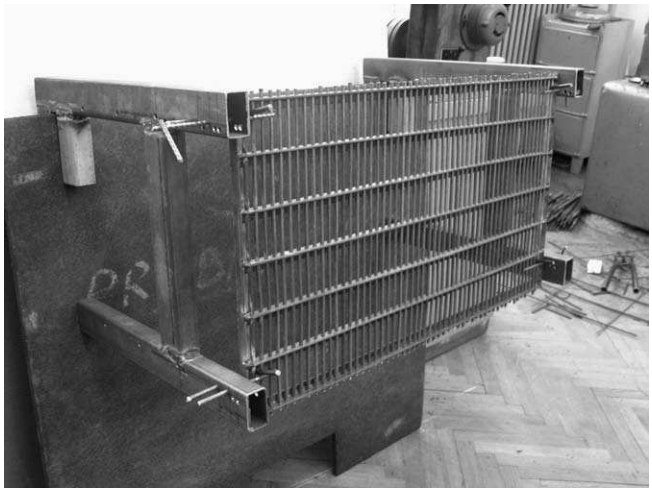

Fig. 1. The applique armour fence setup (parallel wires, PSV, PS20).

The present work was carried out as a part of a continuing programme at the University of Novi Sad, in collaboration with the Military Technical Institute – Belgrade to study and develop different types of ballistic protection systems for the defence industry.

2. Experimental

Chemical composition of patented wire used in this study is given in Table 1. The add-on armour models were made by using patented wires with a diameter of 5 mm. They were suspended in a welded L-profile frame. Tensile properties of patented wire were obtained by using a tensile testing machine VEB ZDM 5/91 with a maximum tensile force of 49,050 N. Average yield strength (YS, 0.2% off set line) of the patented wire used is 1410 MPa, ultimate tensile strength (UTS) is 1630 MPa, elongation (A) is 9.5%, and maximum contraction in radial direction (Z) is 48%.

Applique armour model dimensions were: width 700 mm and height 400 mm. 53 vertical patented wires were placed through drilled holes in horizontal L-profiles (15×15 mm). The whole package was welded to a L-profile welded frame. Two different applique armour models were prepared: the first with holes drilled in a parallel pattern, as shown in Fig. 1, with 12.5–13 mm distances between them, leaving 8–8.5 mm spaces between the wire bodies, and the other, as shown in Fig. 2, with a zig-zag pattern where every other wire is 4 mm closer to the incoming projectile. Both applique model armours were attached to the basic plate by means of two steel frames at the maximum distance of 400 mm (Fig. 1). This basic RHA plate, at 0° from vertical, protects from 7.92 mm SmK (*Spitzgeschoss mit Kern*) hardened steel core [13].

For testing, the following applique model armours were used:

- parallel wire arrangement, stiff mounting, vertical position, 90° from the incoming projectile (marked as PSV, Fig. 1 and 3a),
- parallel wire arrangement, stiff mounting, vertical position, but at 20° measured in vertical plane and 70° from the incoming projectile (PS20), see (Fig. 3b),
- zig-zag wire arrangement, stiff mounting, vertical position, 90° from the incoming projectile (ZSV, Figs. 2 and 3c), and
- zig-zag wire arrangement, free hanging with initial vertical position, 90° from the incoming projectile (ZHV) (Fig. 3d).

In Fig. 4 the hanging mounting of the fence (ZHV) is shown. The fence was hung by two rings each with a diameter of 100 mm, made of rebar with a wire diameter of 5 mm. These rings were supported under a 25 mm bar, firmly mounted by using two U-shaped hooks, over the frames used for armour model mounting in previous tests.

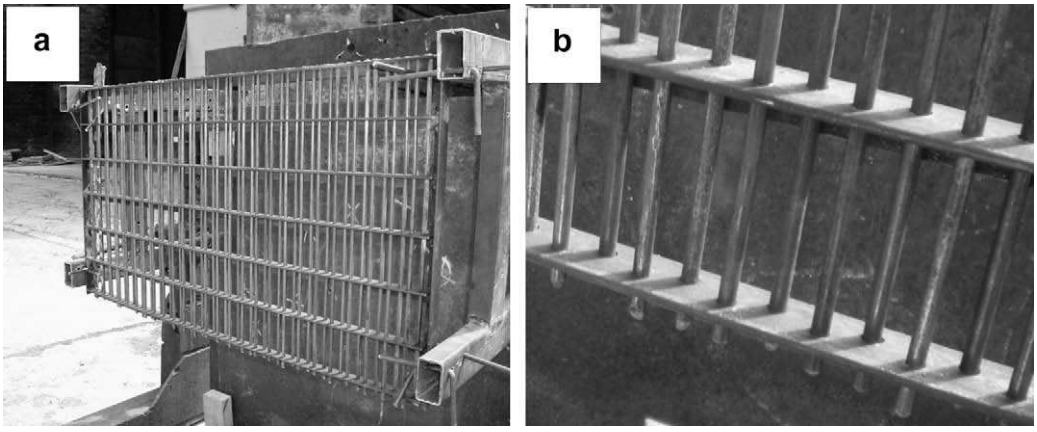

Fig. 2. Zig-zag wire target: (a) ZSV target setup and (b) zig-zag wire setup detail.

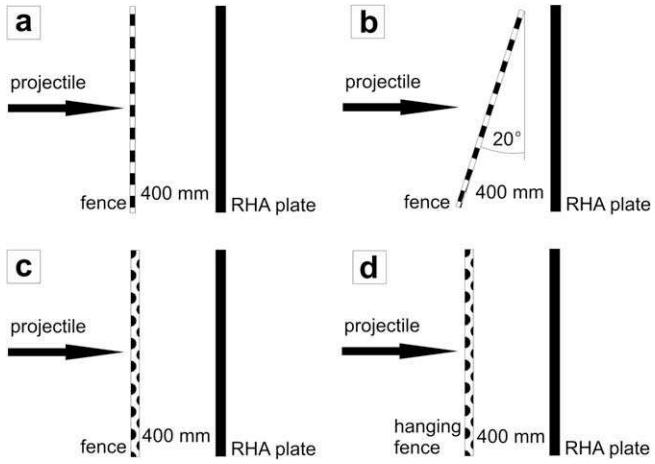

Fig. 3. Test setup of four applique armour models, viewed from above: (a) PSV, (b) PS20, (c) ZSV and (d) ZHV.

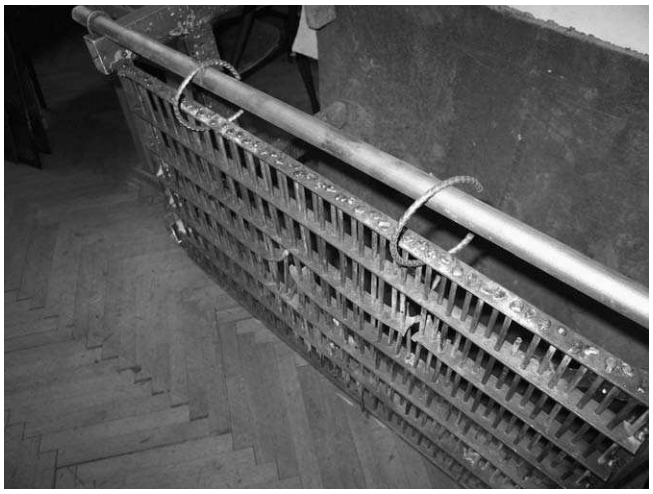

Fig. 4. Hanging setup of the ZHV target.

Ballistic testing was performed by using M8 API ammunition. This ammunition was used in accordance with the standard procedures described in the 1985 Technical regulations for RHA plate acceptance [13]. Steel core hardness was 51 HRc, with a diameter of 10.9 mm, a length of 47.2 mm long and a weight of 24.6 g. This ammunition was fired from a Browning M2HB 12.7 × 99 mm heavy machine gun placed on a tripod, from a 100 m distance. Five shots were fired at each applique armour model.

Muzzle velocity was measured by a BS-850 muzzle velocity radar, at 10 m from the muzzle and compared to the technical regulations for RHA plate acceptance [13]. According to these regulations, muzzle velocity of a M8 API round fired from a Browning M2HB is 910 ± 15 m/s, or 895–925 m/s. From the measured muzzle velocities, and M2 Browning machine gun Firing Tables Charts [14–16], an equivalent firing distance was found:

$$X_e = 100 + X' \tag{1}$$

where X_e (m) is the equivalent distance, 100 refers to 100 m which is the true firing distance, and X' (m) is the distance that corresponds to the measured muzzle velocity [14–16].

Description of fence damage may give indication where the projectile impacted. Description of target damage was carried out according to STANAG 4146 [17]. The obtained results of basic plate damage on its front and back sides were correlated with the impact point on the wire fence, as well as the equivalent firing distance.

Fracture surfaces were examined by JEOL JSM-6460LV scanning electron microscope (SEM), operating at 20 kV. Furthermore, energy dispersive X-ray analysis (EDX) was performed, using an Oxford Instruments INCA Microanalysis system.

3. Results

Description of target damage was carried out according to STANAG 4146 [17]. In this paper, only three relevant descriptions were found:

1. Hole normal (HN) – A complete hole through the plate of approximately the diameter of the projectile
2. Cracked bulge (CB) – A bulge on the back of the plate with at least one distinct crack on it

Table 2
PSV target results.

No.	v_{10} (m/s)	Equivalent firing distance (m)	Attack angle on the fence (°)	Description of fence damage	Attack angle on the basic plate (°)	Description of basic plate damage
PSV-1	842.2	210	0	One wire impacted, deformed and ripped out of the frame	0	Cracked bulge
PSV-2	867.3	155	0	Two wires impacted and similarly deformed	0	Hole normal
PSV-3	857.1	191	0	One wire impacted, deformed and broken	0	Cracked bulge
PSV-4	862.0	173	0	One wire impacted, deformed and fractured	0	Cracked bulge, the dent over PSV1
PSV-5	884.4	137	0	One wire impacted, deformed and fractured	0	Cracked bulge

Table 3
PS20 target results.

No.	v_{10} (m/s)	Equivalent firing distance (m)	Attack angle on the fence (°)	Description of fence damage	Attack angle on the basic plate (°)	Description of basic plate damage
PS20-1	854.5	209	20	Two wires impacted and similarly deformed	0	Cracked bulge (two cracks)
PS20-2	865.0	173	20	One wire impacted, deformed and fractured	0	Smooth bulge
PS20-3	864.1	174	20	One wire impacted, deformed and fractured	0	Cracked bulge
PS20-4	859.4	192	20	One wire impacted, deformed and fractured	0	Cracked bulge
PS20-5	862.3	180	20	Two wires impacted and similarly deformed	0	Cracked bulge (two cracks)

Table 4
ZSV target results.

No.	v_{10} (m/s)	Equivalent firing distance (m)	Attack angle on the fence (°)	Description of fence damage	Attack angle on the basic plate (°)	Description of basic plate damage
ZSV-1	871.6	147	0	One wire impacted, deformed and fractured	0	Hole normal
ZSV-2	874.2	145	0	One wire impacted, deformed and fractured	0	Cracked bulge
ZSV-3	884.4	137	0	One wire impacted, deformed and fractured	0	Cracked bulge
ZSV-4	874.8	145	0	One wire impacted, deformed and fractured	0	Smooth bulge – core fractured in two parts
ZSV-5	876.1	144	0	Two wires impacted and similarly deformed	0	Cracked bulge

Table 5
ZHV target results.

No.	v_{10} (m/s)	Equivalent firing distance (m)	Attack angle on the fence (°)	Description of fence damage	Attack angle on the basic plate (°)	Description of basic plate damage
ZHV-1	872.7	146	0	One wire impacted, deformed and fractured	0	Smooth bulge
ZHV-2	892.8	110	0	Two wires impacted and similarly deformed	0	Cracked bulge
ZHV-3	880.5	140	0	One wire impacted, deformed and fractured	0	Cracked bulge
ZHV-4	878.5	142	0	Two wires impacted and similarly deformed	0	Cracked bulge
ZHV-5	890.1	112	0	One wire impacted, deformed and fractured	0	Cracked bulge

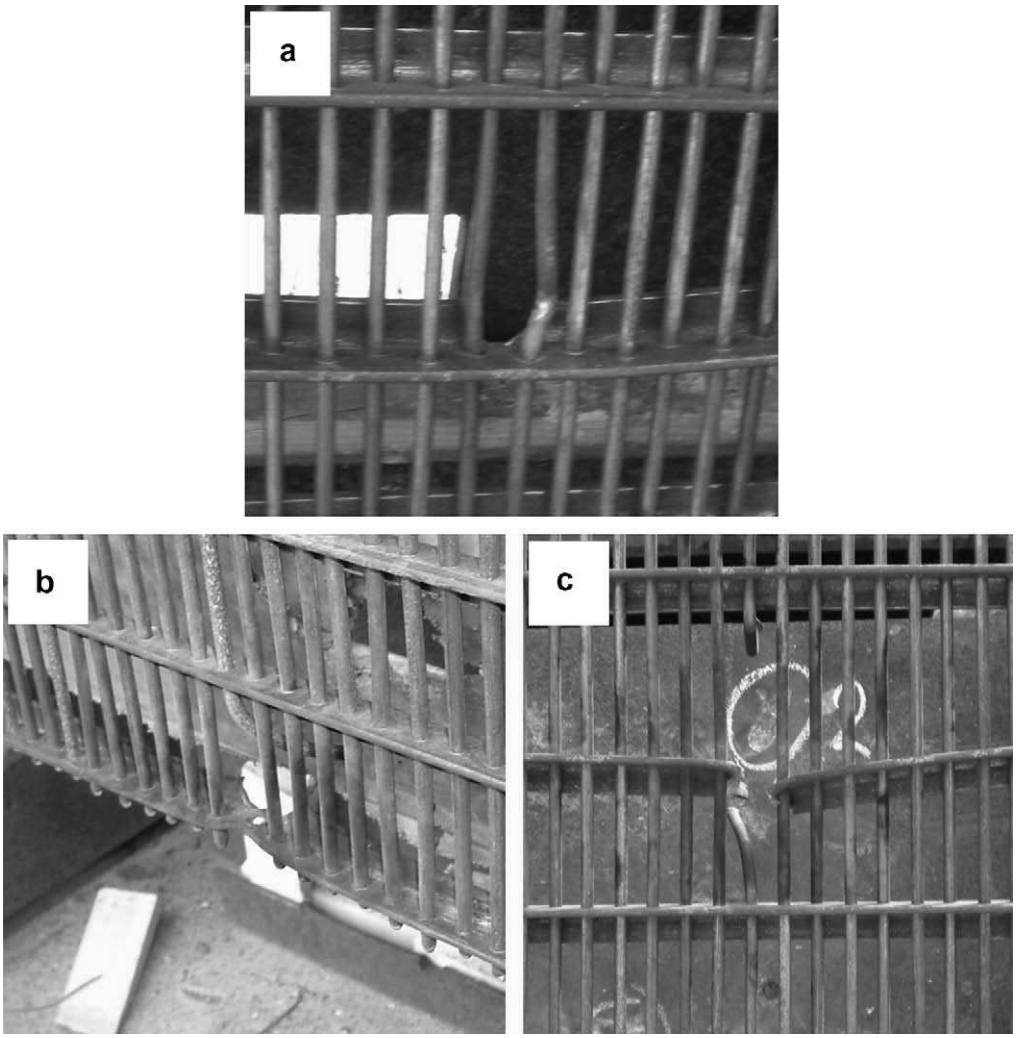

Fig. 5. Damage on the fence: (a) two wires impacted and similarly deformed (ZHV-2), (b) one wire impacted, deformed and ripped out of the frame (PSV-1) and (c) one wire impacted, deformed and fractured (ZSV-2).

3. Smooth bulge (SB) – A bulge on the back of the plate without cracks

The results for various applique armour models are given in Tables 2–5. Muzzle velocities vary from 842.2 to 892.8 m/s, which is outside of the range of standard value of 895–925 m/s listed in the 1985 Technical regulations for RHA plate acceptance [13]. Therefore, equivalent firing distances were given for each shot, calculated according to Eq. (1). From Tables 2–5, it can be noticed that the equivalent firing distances were from 110 to 210 m. Damage on the fence as the result of projectile impact can be classified into three categories: two wires impacted and similarly deformed (Fig. 5a); one wire impacted, deformed and ripped out of the frame (Fig. 5b); one wire impacted, deformed and fractured (Fig. 5c). Dark marks on surrounding wires (Fig. 5) are the result of the incendiary effect of API ammunition. Damage on the basic rolled homogenous armour (RHA) plate can be classified in three categories as well: hole normal, cracked bulge and smooth bulge, where two types of cracked bulge occured, one with one crack and the other with two cracks (Fig. 6a–d).

In Fig. 7, two impacts of API penetration core (PSV-1 and PSV-4) on the basic RHA plate face are shown. Two cores impacted sideways as the result of passing through the wire fence. In Figs. 7 and 8 (impact marked as 3-ZSV-3) a typical elongated dent on the RHA plate face are shown, as the result of sideways impact on the RHA plate. However, in Fig. 8, the dent marked as 1 (ZSV-1) shows the penetration that still occured, as the result of

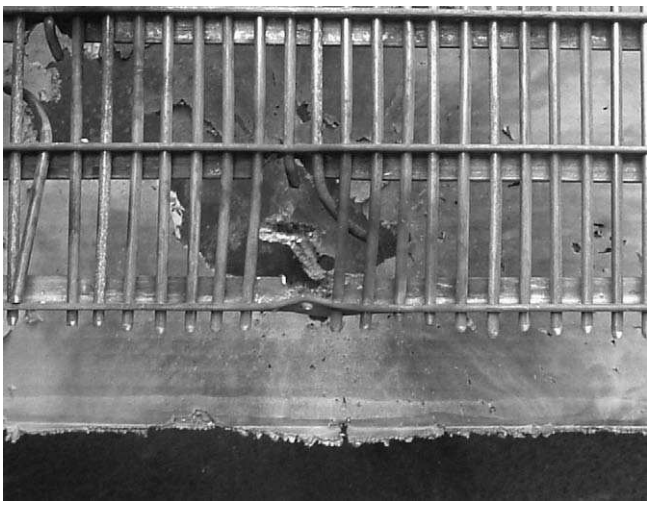

Fig. 7. Elongated dents one over the other (PSV-4 and PSV-1).

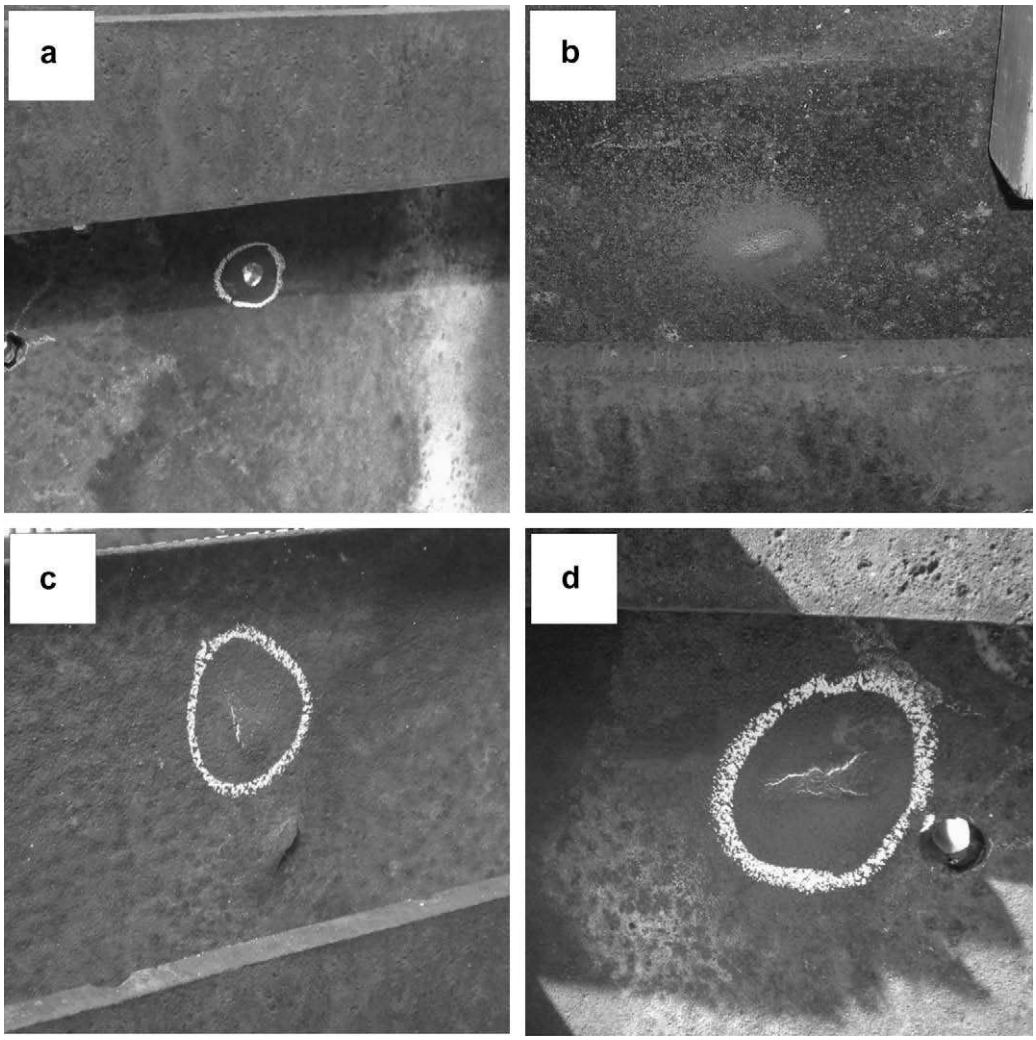

Fig. 6. Damage on the RHA plate back surface: (a) hole normal (PSV-2), (b) cracked bulge and smooth bulge (PS20-2), (c) where two types of cracked bulge occured (ZSV-2) and (d) one with one crack and the other with two cracks (PS20-1).

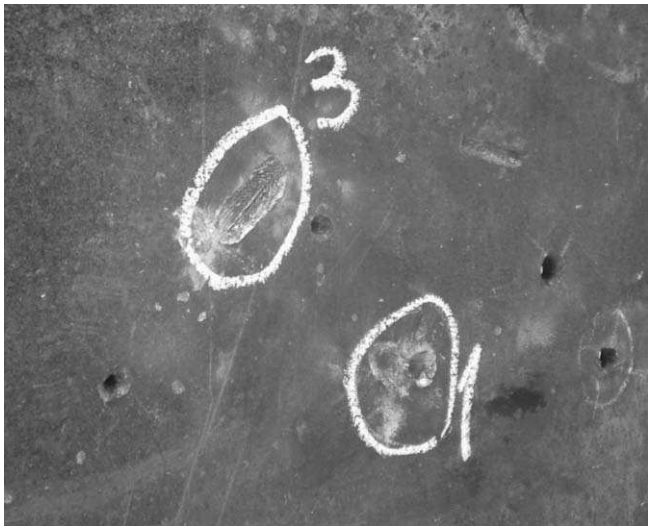

Fig. 8. ZSV-3 (marked as 3) and ZSV-1 (marked as 1).

Fig. 10. Fractured core of M8 API ammunition used in PS20-2.

an insufficient yaw angle – the dent is elongated, but with a penetration that nevertheless occured. In Fig. 9, there are two distinct damage levels on the fence – in both cases the projectile impacted one wire, but on various heights in relation to the mild steel frame. Furthermore, in Fig. 9a (ZSV-4), the fractured wire can be found along with damage to one part of the horizontal segment of the frame, while in Fig. 9b (PS20-2), only the vertical wire that was fractured can be seen. As the result of previous fence impact, the core of the projectile may even fracture (Fig. 9a). This is also shown in Fig. 10, where the M8 API penetrating core was extracted with a clearly visible crack that has not propagated through the whole cross-section of the core (PS20-2).

Sem fractograhs are shown in Fig. 11a–d. Two regions are identified, smooth central and coarse peripheral. EDX analysis indicated that the fracture surface is covered by debris, which may be the result of incendiary effect and jacket particles of ammunition used, Fig. 12.

4. Discussion

It can be noticed that when two wires were impacted and similarly deformed, Fig. 5a, as in case of PSV-1 (Table 2), the projectile impacted approximately between two wires, with approximately the same region of its *ogival* front portion. Two wires were similarly deformed in other cases: PS20-1 and PS20-5 (Table 3), ZSV-5 (Table 4) and ZHV-2 and ZHV-4 (Table 5). In the first two cases, PS20-1 and PS20-5, muzzle velocity was lower than in case of PSV-1, while in case of the ZSV-5, ZHV-2 and ZHV-4, muzzle velocity was higher. In none of these cases penetration occured. The most severe damage – crack bulge – was noticed in PS20-1 and PS20-5. The main reason for this phenomenon may be the angled position of the add-on fence or a more complex arrangement of the wires, which prevents the projectile from impacting two wires simultaneously and therefore, provides a more effective destabilization of the core. Furthermore, in the last two cases, ZHV-2 and ZHV-4, that refer to the free hanging arrangement, the damage level of the basic plate is lower – cracked bulge with one rather than with two cracks. The main reason for this may be the energy dissipation of the projectile that hits a hanging target.

Other cases of fence damage refer to the case when one wire was impacted, deformed and fractured. Obviously, this case brings the most effective disturbance of the projectile, forcing it to strike the main RHA plate sideways. This caused different basic plate damage levels, smooth bulge and cracked bulge. In the case of PSV-4 (Table 2), the cracked bulge occured, with a dent over the PSV-1 dent, indicating a considerable multi hit – capability, Fig 6. According to the 1985 Technical regulations for RHA plate acceptance [13], a strike that is within two diameters of the previous hit or dent is not valid due to the fact that the material

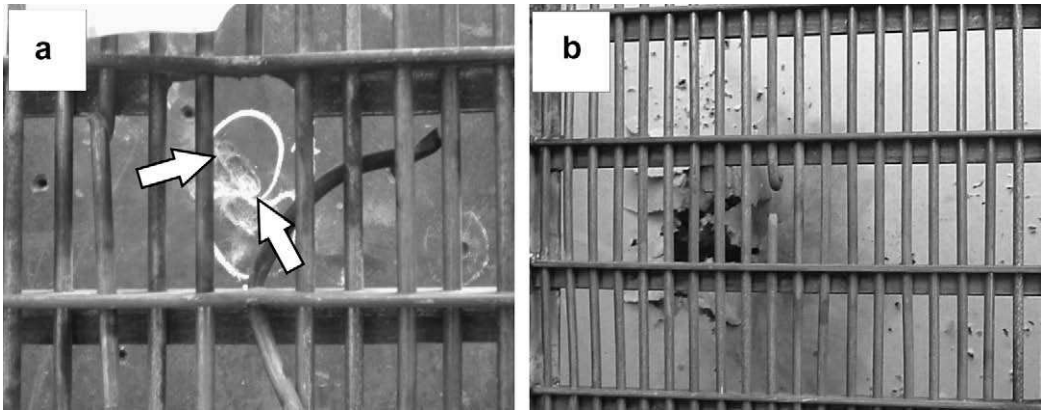

Fig. 9. Damage on the fence: (a) ZSV-4 and (b) PS20-2.

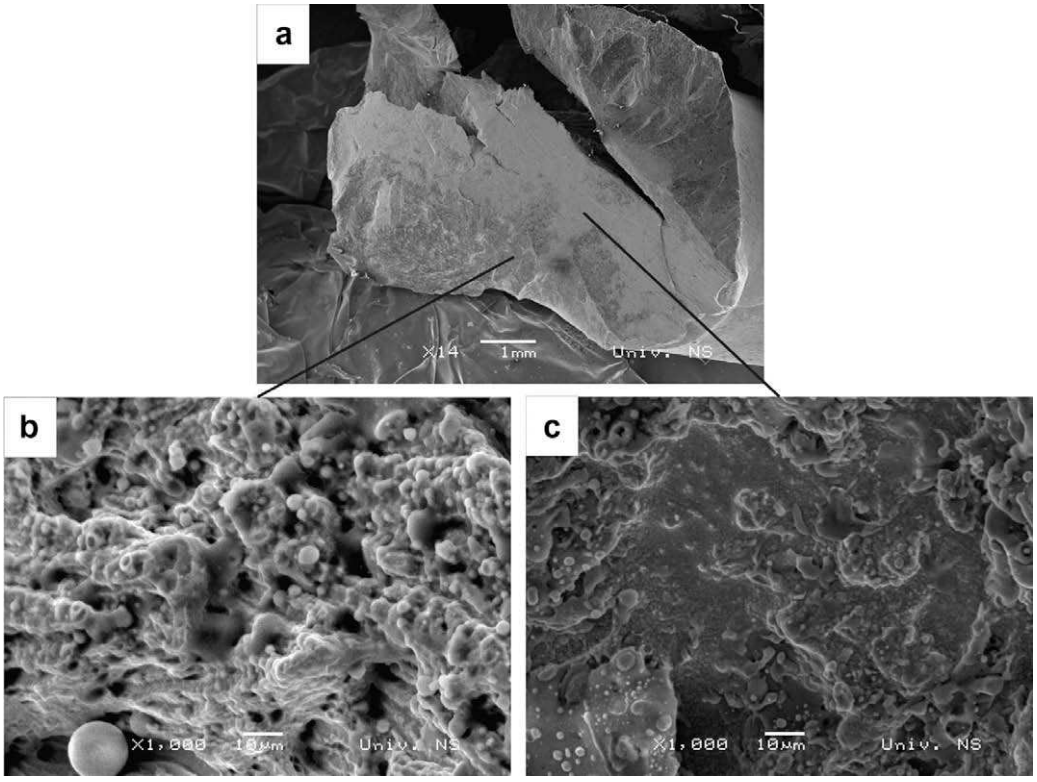

Fig. 11. SEM fractographs showing: (a) macro image, (b) smooth central region, (c) central region debris and (d) peripheral region with thinner debris layer revealing dimples.

is weakened in this zone. However, in case of ZSV-1, when one wire was impacted, deformed and fractured, a normal hole occured (penetration). No damage or dent was noticed on the point of impact, similar to other cases where the penetrating core impacted the basic RHA plate sideways, indicating that the yaw of the projectile, in this case, was minimal (Fig. 7). The most probable point of impact was very close to the center of the wire, which caused an insufficient disturbance or yaw of the penetrating core.

In the case of ZSV-4, the projectile impacted one wire, deformed and fractured it. However, the resulting damage on the basic RHA plate revealed not one elongated dent (Fig. 7) that occurs on other occasions (smooth and cracked bulge), but two (Fig. 8a). These two dents appear to be as one. However, there are clearly two very close dents with two depressions in the basic RHA plate. There is no evidence that the penetrating core of the projectile fractures after the impact on the patented wire, continuing towards the basic RHA plate in two pieces. Such a phenomenon occurs as the result of the bending stresses that are induced by edge impact [18]. The core, must be made of steel with a very high hardness, because it is necessary to provide the needed rigidity during the penetration process. However, it inevitably has low ductility. Therefore, such a core may be broken if a sufficiently hard and rigid edge is impacted. An answer to this occurence may be given by analyzing one recovered penetrating core (PS20-2), with an obvious crack that has not propagated through the whole cross-section of the core (Fig. 9). Such a crack developed after the impact into RHA plate. This indicates that on other occasions (such as ZSV-4), a similar crack may have propagated through the whole cross-section. If the damage levels on the fence of PS20-2 and ZSV-4 are compared (Fig. 8a and b), it might be noted that it is more severe on ZSV-4, since a portion of the mild steel frame has been damaged. However, ZSV-4 is an "exception to the rule", due to the fact that only 30.5% of the add-on armour model is covered in mild steel L-profiles that may, in conjunction with the patented wire, offer a sufficiently rigid target.

Macro images shown in Figs. 5, 7 and 9 show severe wire bending deformation, indicating a ductile fracture mode. SEM micrographs of fracture surfaces show the existence of two regions, smooth surface in the center and coarse radial marks at the edges, Fig. 11a. In Fig. 11b–d, it can be seen that the surface is irregular and covered with a layer, which was confirmed by EDX analysis. It was found that the layer consists of copper, barium, aluminium and magnesium, Fig. 12. These elements come from the projectile jacket (copper) and incendiary mixture: IM-11 consists of 50% barium-nitrate $Ba(NO_3)_2$ and 50% magnesium–aluminium alloy [19]. In the central region, Fig. 11b and c, under the debris layer may be a smooth surface which may be the result of heavy shear deformation of dimples along the direction of shear stress. However, at peripheral region, the debris layer is obviously thinner (Fig. 11d) revealing dimples indicating a ductile fracture mode. The size and distribution of larger dimples seen in Fig. 11b closely corresponds to the dimples found on fracture surfaces of tensile and impact tested samples of the same material, Fig. 13a and b.

This fence, made from high strength patented wire and mild steel L-profiles, had a weight of 6765 g, or an areal density of 24.16 kg/m^2 (PSV, ZSV and ZHV applique armour models), while for the inclined PS20, areal density was 25.71 kg/m^2. The basic RHA plate had an areal density of 102.05 kg/m^2, while the areal density of the combined basic RHA plate with the fence was 126.21 kg/m^2, or an equivalent of a RHA steel plate 16.08 mm thick. According to the 1985 Technical regulations for RHA plate acceptance [13], an RHA plate that offers protection from M8 API ammunition fired from a Browning M2HB machine gun has an areal density of 211.95 kg/m^2. With armour models PSV, ZSV and ZFV, mass efficiency of the whole RHA and applique armour model was 1.68, while for PS20, due to the inclination of the fence, the mass efficiency was 1.58.

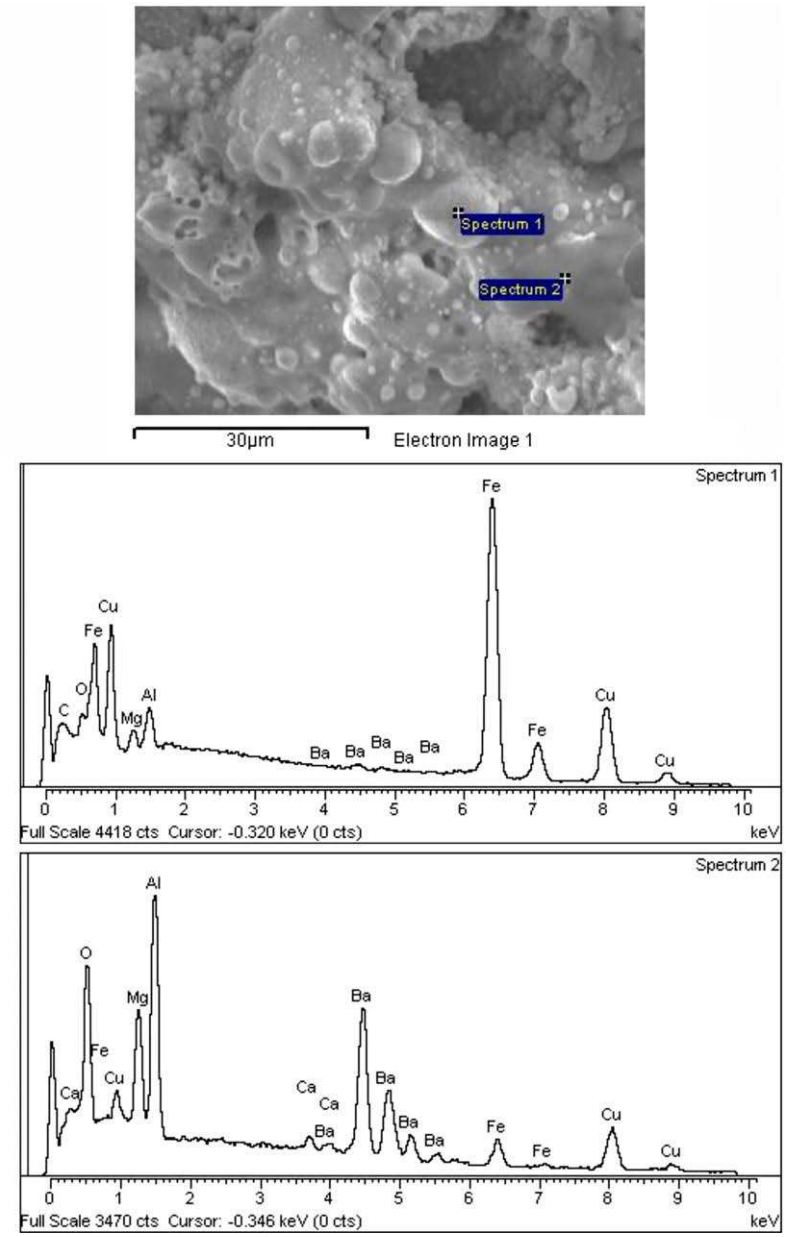

Fig. 12. EDX analysis results.

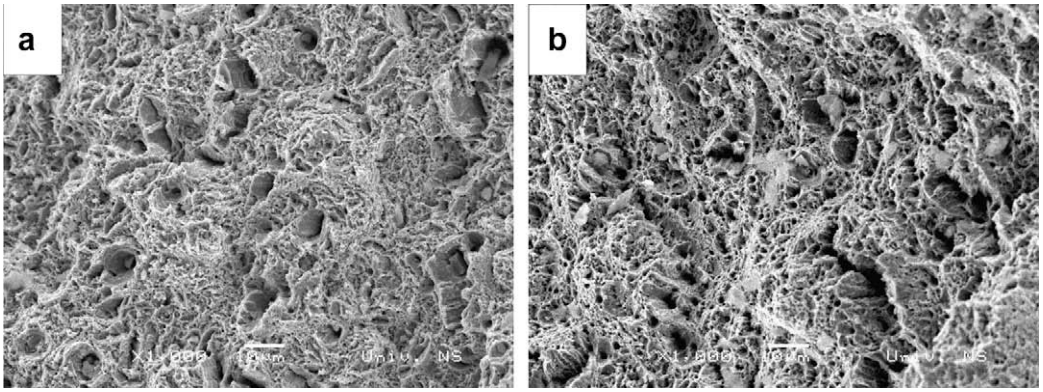

Fig. 13. Fracture surfaces of tensile (a) and impact (b) tested samples of patented wire.

5. Conclusions

According to the obtained results, some conclusions may be drawn. Patented wire has shown great potential as a basis for a fence applique armour. It is very attractive not only due to its availability, but also because it has a very effective yaw-inducer. A penetrating core of 12.7 mm M8 API ammunition at a high yaw angle was not capable of penetrating the basic 13 mm RHA plate, even when a core made an impact over the previous one, demonstrating a higher multiple-impact capability than found on homogenous armour types. Equivalent firing distance, if between 110 and 210 m has no effect on the performance of tested applique armour models.

In addition, for each applique armour model separate conclusions are presented:

- PSV applique armour model has shown a limitation of offering a very questionable efficiency in disturbing the penetrating core in the case of impact between two wires. When this occurs, the impact is performed by approximately the same portion of the *ogival* front of the penetrating core by moving the wires apart without sufficient momentum reduction.
- PS20 and ZSV are basically very similar applique armour models. Wire arrangement, without parallel wires, efficiently prevents the penetrating core to impact two wires at approximately the same time, with a similar *ogival* portion. Although PS20 prevented all projectiles to penetrate the basic RHA plate, ZSV did not. However, PS20 has not suffered approximately direct impact into one wire, which results in an un sufficient induced yaw, so the penetrating core is not been sufficiently disturbed. As such, the core penetrates the basic RHA plate.
- It is unclear what would have been the effect of the approximate direct impact on the wire of the ZHV applique armour model. However, it has been noticed that the damage effects on the basic RHA plate are less pronounced, for a similar type of damage on the fence, which may be the result of a higher energy loss of the projectile absorbed by the fence itself while moving after each impact.

If the efficiency of the applique armour is considered to be the highest priority, ZHV applique armour model has shown the highest potential. However, a ZSV – like armour with zig-zagged wires is probably the most convenient compromise between efficiency and ease of mounting on an actual armoured vehicle.

Acknowledgements

The authors would like to thank Mr. Jeff Duquette for overall support and useful suggestions in determining a correct terminology of steel RHA steel plate damage. Furthermore, the authors would like to thank Ms. Margareta Lela for English language corrections.

References

[1] Kemp I, Biass EH. The trend, Armada international – complete guide, 2006; 1: 1-32.
[2] Doyle D. Gun trucks in vietnam 1. Classic Military Veh 2008;80:20–3.
[3] Doyle D. Gun trucks in vietnam 2. Classic Military Veh 2008;81:24–7.
[4] Williams AG. Rapid fire. Shrewsbury: Airlife Publishing Ltd.; 2000. p. 342.
[5] Hogg IV, Weeks J. Military small arms of 20th century. Wausau: Krause Publication Inc,; 2000. p. 240.
[6] Goldsmith W. Review: non-ideal projectile impact on targets. Int J Impact Eng 1999;22:95–395.
[7] Phelps W, Schoeters R. Panzer IV survivors: Ausf. A-J. Self published; 2005. p. 75.
[8] Jenz T, Doyle H. Drachtgeflectschuerzen. AFV News May-August 2002;37:6–8.
[9] Chen S, Wang X, Jia Y. A comparative study of continuous steel-concrete composite beams prestressed with external tendons: experimental investigation. J Construct Steel Res 2009;65:1480–9.
[10] Toribio J, Valiente A. Failure analysis of cold drawn eutectoid steel wires for prestressed concrete. Eng Fail Anal 2006;13:301–11.
[11] Edwards MR, Mathewson A. The ballistic properties of tool steel as a potential improvised armour plate. Int J Impact Eng 1997;19:297–309.
[12] Borvik T, Dey S, Clausen AH. Perforation resistance of five different high-strength steel plates subjected to small-arms projectiles. Int J Impact Eng 2009;36:948–64.
[13] SNO 1645 Pancirni lim od celika HPA-10. Technical regulations for RHA plate acceptance; 1985. p. 11.
[14] FT 0.50-H-1 Firing tables, gun, machine M2; 1942. p. 51.
[15] Wardepartment FM 23-65 Basic Field Manual. Browning Machinegun, Caliber .50 M2. Washington, USA: Government Printing Office; 1940. p. 42.
[16] SSNO TS I-I/I, M715; 1974. p. 92.
[17] STANAG 4146 Annex D; 1998. p. D-1.
[18] Chocron S, Anderson Jr CE, Grosch DJ, Popelar CH. Impact of the 7.62 mm APM2 projectile against the edge of a metallic target. Int J Impact Eng 2001;25:423–37.
[19] SSNO TS I-I/I, M715; 1974. p. 97.